The Plant Cell, Vol. 25: 3841–3857, October 2013, www.plantcell.org

The *Arabidopsis* Eukaryotic Translation Initiation Factor eIF5A-2 Regulates Root Protoxylem Development by Modulating Cytokinin Signaling[W]

Bo Ren,[a,1] Qingguo Chen,[a,b,1] Sulei Hong,[a,b] Wenming Zhao,[a,b] Jian Feng,[a,b] Haizhong Feng,[a] and Jianru Zuo[a,2]

[a] State Key Laboratory of Plant Genomics and National Plant Gene Research Center, Institute of Genetics and Developmental Biology, Chinese Academy of Sciences, Beijing 100101, China

[b] University of Chinese Academy of Sciences, Beijing 100049, China

The phytohormone cytokinin regulates various aspects of plant growth and development, including root vascular development. In *Arabidopsis thaliana*, mutations in the cytokinin signaling components cause misspecification of protoxylem cell files. Auxin antagonizes cytokinin-regulated root protoxylem differentiation by inducing expression of *ARABIDOPSIS PHOSPHOTRANSFER PROTEIN6* (*AHP6*), a negative regulator of cytokinin signaling. However, the molecular mechanism of cytokinin-regulated protoxylem differentiation is not fully understood. Here, we show that a mutation in *Arabidopsis FUMONISIN B_1-RESISTANT12* (*FBR12*), which encodes a eukaryotic translation initiation factor 5A, causes defective protoxylem development and reduced sensitivity to cytokinin. *FBR12* genetically interacts with the cytokinin receptor *CYTOKININ RESPONSE1* (*CRE1*) and downstream *AHP* genes, as double mutants show enhanced phenotypes. FBR12 forms a protein complex with CRE1 and AHP1, and cytokinin regulates formation of this protein complex. Intriguingly, *ahp6* partially suppresses the *fbr12* mutant phenotype, and the *fbr12* mutation causes increased expression of *AHP6*, indicating that *FBR12* negatively regulates *AHP6*. Consistent with this, ectopic expression of *FBR12* in the *CRE1*-expressing domain partially rescues defective protoxylem development in *fbr12*, and overexpression of *AHP6* causes an *fbr12*-like phenotype. These results define a regulatory role of the highly conserved FBR12 in cytokinin-mediated root protoxylem specification.

INTRODUCTION

In higher plants, the radial pattern of a root contains, from outside to inside, the epidermis, the cortex, the endodermis, the pericycle, and the central vascular cylinder. The root vascular bundles consist of xylem and phloem with intervening procambial cells and surrounding pericycle cells. The root vascular tissue forms from undifferentiated procambial cells during embryogenesis and differentiates as the phloem and xylem strands (Steeves and Sussex, 1989; Dolan et al., 1993). In the mature zone of an *Arabidopsis thaliana* root, the xylem axis contains two opposite-oriented protoxylem cells adjacent to the pericycle layer. Protoxylem has a characteristic helical, thickened cell wall. Across the central axis, metaxylem forms at the inner side of protoxylem at a later developmental stage, and the phloem cell files form perpendicular to the xylem axis. Xylem and phloem are separated by intervening procambial cell files, which form cambium during secondary development by periclinal cell divisions (Steeves and Sussex, 1989; Dolan et al., 1993; Fukuda, 2004).

The phytohormone cytokinin plays a key role in the complex mechanism regulating root xylem development (Mähönen et al., 2000, 2006b; Bishopp et al., 2011a, 2011b). Cytokinin signaling is mediated by a two-component system, involving in a phosphorelay that functions by sequential transfer of phosphoryl groups from receptors to downstream components (Hwang and Sheen, 2001; To and Kieber, 2008; Werner and Schmülling, 2009; Hwang et al., 2012). *Arabidopsis* has three characterized cytokinin receptors, the His kinases, CYTOKININ RESPONSE1 (CRE1)/WOODEN LEG (WOL)/ARABIDOPSIS HISTIDINE KINASE4 (AHK4), AHK2, and AHK3. Downstream of these receptors, phosphotransfer proteins (ARABIDOPSIS PHOSPHOTRANSFER PROTEIN1 [AHP1] through AHP5) transfer the phosphoryl group from the receptor to the downstream targets. Transfer of the phosphoryl group from AHPs activates the type-B response regulators (ARRs), a group of MYB-class transcription factors, which then promote the expression of type-A *ARRs* and other targets. Type-A ARRs, in turn, negatively regulate the phosphorelay, thus forming a feedback regulatory loop. Interestingly, the CRE1 receptor has kinase activity when bound to cytokinin, but in the absence of cytokinin, CRE1 acts as a phosphatase on AHPs (Mähönen et al., 2006a). The stability of type-B ARR proteins is negatively regulated by the 26S proteasomal degradation machinery, mediated by an F-box E3 ubiquitin ligase KISS ME DEADLY (Kim et al., 2012, 2013).

Mutations in several components of the cytokinin signaling pathway cause impaired vascular development. In particular, the *wol* mutation and the *ahk2 ahk3 ahk4* triple receptor mutations

[1] These authors contributed equally to this work.

[2] Address correspondence to jrzuo@genetics.ac.cn.

The author responsible for distribution of materials integral to the findings presented in this article in accordance with the policy described in the Instructions for Authors (www.plantcell.org) is: Jianru Zuo (jrzuo@genetics.ac.cn).

[W] Online version contains Web-only data.

www.plantcell.org/cgi/doi/10.1105/tpc.113.116236

result in the transformation of all cell files of the root vascular cylinder into protoxylem (Mähönen et al., 2000, 2006b; Higuchi et al., 2004; Nishimura et al., 2004). Defective xylem development was also observed in an *ahp1,2,3,4,5* quintuple mutant (Hutchison et al., 2006) and, in a lesser extent, in an *arr1 arr10 arr12* triple mutant of type-B *ARR* genes (Argyros et al., 2008; Ishida et al., 2008). Consistent with these observations, tissue-specific depletion of endogenous cytokinins in the *CRE1/AHK4*-expressing domain causes a similar phenotype (Mähönen et al., 2006b). Conversely, mutations in *AHP6*, which encodes a pseudophosphotransfer protein that acts as a negative regulator of cytokinin signaling, cause reduced protoxylem cell files (Mähönen et al., 2006b). These observations led to the proposal that reciprocal interactions of the phosphorelay and AHP6 modulate cell proliferation and cell differentiation during root vascular development. Vascular cell fate determination in the absence of cytokinin signaling may default to protoxylem formation (Mähönen et al., 2006b).

The interaction between cytokinin and auxin coordinates root growth and development in response to environmental and internal cues (Müller and Sheen, 2008; Bishopp et al., 2011a, 2011b). In particular, auxin and cytokinin form a mutually-inhibitory feedback loop, in which cytokinin modulates the bisymmetric distribution of the PIN-FORMED (PIN) auxin efflux proteins, and auxin, in turn, promotes *AHP6* transcription, which terminates the loop. This reciprocal inhibition between auxin and cytokinin plays an important role in specifying vascular pattern in the root meristem (Bishopp et al., 2011a, 2011b).

In addition to signaling mediated by phytohormones, several transcription factors also regulate protoxylem specification. Overexpression of *VASCULAR-RELATED NAC-DOMAIN7* (*VND7*) causes the transformation of stele cells into protoxylem by regulating expression of genes for xylem vessel formation (Kubo et al., 2005; Yamaguchi et al., 2011). Moreover, mutations in *LONESOME HIGHWAY* (*LHW*), a helix-loop-helix transcription factor gene expressed in the root meristem, result in fewer cells inside the stele and the production of only one strand of xylem and phloem cell files (Ohashi-Ito and Bergmann, 2007). This phenotype, however, does not fit with the model that cytokinin promotes cell divisions of the stele and inhibits protoxylem differentiation, thus raising the possibility that *LHW* may act independent from cytokinin signaling (Ohashi-Ito and Bergmann, 2007).

In this study, we revealed a regulatory role of eukaryotic translation initiation factor 5A-2 (eIF5A-2) in root protoxylem development. eIF5A was initially identified as a translation initiation factor from rabbit reticulocyte lysates, and eIF5A proteins are highly conserved in eukaryotes and archaea (Kemper et al., 1976). Several studies suggest that in vivo protein synthesis does not require eIF-5A (Kang and Hershey, 1994; Park et al., 1997), but recent studies imply that eIF-5A proteins function in the elongation step of translation, rather than in the initiation step as originally proposed (Saini et al., 2009; Ma et al., 2010). In addition, eIF5A plays a role in the regulation of RNA stability and the transport of RNA between the nucleus and the cytoplasm (Bevec and Hauber, 1997; Zuk and Jacobson, 1998; Rosorius et al., 1999; Schrader et al., 2006). The eIF5A proteins also interact with several proteins, likely involved in intracellular trafficking of RNA or proteins (Rosorius et al., 1999; Lipowsky et al., 2000; Hofmann et al., 2001; Thompson et al., 2003; Li et al., 2004). Therefore, eIF5A was proposed to be a bimodular protein capable of binding to both RNA and proteins, thus playing multiple roles in distinctive cellular activities (Thompson et al., 2003; Jao and Chen, 2006). The precise biochemical activity of eIF5A remains to be fully elucidated.

As a highly conserved housekeeping gene, *eIF5A* plays a critical role in growth and development by regulating cell division, cell expansion, cell differentiation, and cell death in a variety of organisms (Thompson et al., 2004). The *Arabidopsis* genome contains three *eIF5A* genes, *eIF5A-1*, *eIF5A-2*, and *eIF5A-3* (Thompson et al., 2004), of which *eIF5A-2*, also known as *FUMONISIN B_1-RESISTANT12* (*FBR12*), represents the major activity of this small gene family (Feng et al., 2007). Mutations in *eIF5A-2* cause severe defects in plant growth and development and eventually seedling lethality (Feng et al., 2007). In addition, *eIF5A* genes regulate stress responses, programmed cell death, stem xylem development, and leaf senescence (Thompson et al., 2004; Feng et al., 2007; Hopkins et al., 2008; Liu et al., 2008b; Ma et al., 2010). In particular, *Arabidopsis eIF5A-1* and *FBR12/eIF5A-2* genes affect stem xylem development (Feng et al., 2007; Liu et al., 2008b). Moreover, a pumpkin (*Cucurbita maxima*) eIF5A occurs in the phloem sap and interacts with phloem proteins, implying a possible role in the regulation of the sieve tube system (Ma et al., 2010). Here, we report a specific activity of *FBR12/eIF5A-2* in root vascular development by modulating cytokinin signaling.

RESULTS

eIF5A Genes in Root Protoxylem Development

The *fbr12* mutant carries a T-DNA insertion in *eIF5A-2* and has no detectable *FRB12* mRNA or FBR12 protein (Feng et al., 2007) (see Supplemental Figure 1 online). We identified a second mutant allele CS852785 in the Columbia-0 (Col-0) background, which showed a similar phenotype (see Supplemental Figures 1 and 2 online). Accordingly, we renamed the original mutant as *fbr12-1* (in the Wassilewskija [Ws] background) and CS852785 as *fbr12-2*. The data presented below were generated based on *fbr12-1*, and we refer to *fbr12-1* as *fbr12* hereafter, unless otherwise indicated.

The *fbr12* mutants had significantly shorter primary roots than wild-type seedlings (Figure 1A). Analysis of the transverse sections of the roots revealed relatively normal cell files in the epidermis and the cortex of the *fbr12* root, compared with the wild-type root. However, the cell linage in the *fbr12* root vascular cylinder was disorganized and had fewer cells and reduced cell files of the intervening procambial cells (Figures 1B and 1C). The phloem cell files remained relatively normal, but extra protoxylem cell files were observed in nearly half of *fbr12* roots (46.9%; Figures 1D and 1E), suggesting that *fbr12* root protoxylem development is impaired by *fbr12*. These developmental defects were fully rescued by an *FBR12* (Feng et al., 2007) or an *FBR12-FLAG* transgene driven by an *FBR12* promoter, but not by an *FBR12^{K51S}* transgene (see Supplemental Figure 3 online). The highly conserved Lys-51 residue of eIF5A is posttranslationally modified by hypusination, which converts Lys into the amino acid

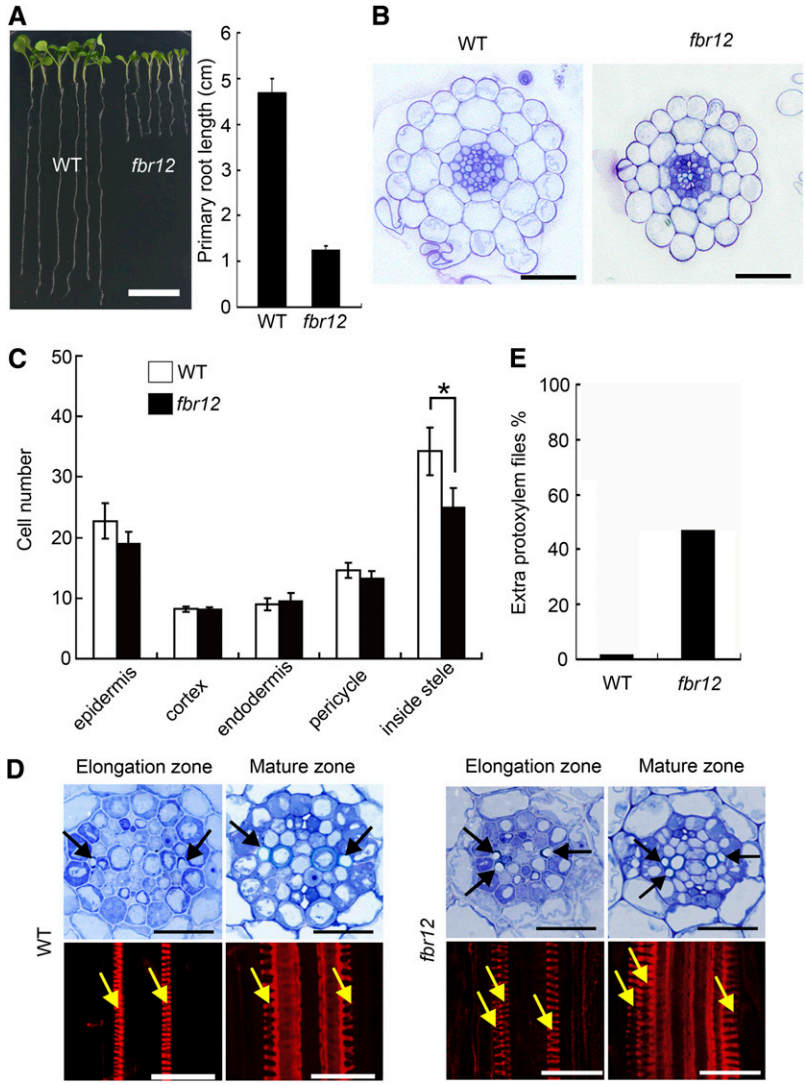

Figure 1. Altered Vascular Development in *fbr12* Roots.

(A) Left: Seedlings of the wild type (WT) and *fbr12*. Right, measurement of the primary root length shown at the left side. The means of three replicates (n = 30) ± SD are shown. Bar = 1 cm.

(B) Transverse sections of wild-type and *fbr12* roots. Bars = 40 μm.

(C) The cell number of different tissues in wild-type and *fbr12* roots (n = 40). Asterisk indicates statistically significant difference (analysis of variance, $P < 0.01$). Bars denote SD.

(D) Protoxylem development in wild-type and *fbr12* roots. **(Top)** Transverse sections. **(Bottom)** Longitudinal images of xylems stained with basic Fuchsin red and visualized under a confocal microscope. Arrows denote protoxylem cell files. Bars = 20 μm.

(E) Quantitative analysis of the extra protoxylem phenotype in wild-type and *fbr12* roots (n = 40).

Eight-day-old seedlings were used in all the experiments.

hypusine. This unique modification is essential for the activity of eIF5A proteins (Park et al., 1997; Thompson et al., 2004).

To explore the possible roles of the three *Arabidopsis eIF5A* genes in root xylem development, we first analyzed their expression patterns by generating transgenic plants carrying promoter:*GUS* (β-glucuronidase) reporter genes. We detected weak expression of *eIF5A-1*:*GUS* in the vascular tissue of the maturation zone of the root and the anther (Figure 2A). In the *eIF5A-2*/*FBR12*:*GUS* transgenic plants, we detected GUS activity in most organs and tissues (Figure 2B). The root showed most GUS activity inside the stele of the mature zone, where the maturation of protoxylem occurs (Figures 2B). We confirmed this expression pattern by immunostaining root transverse sections using an anti-FBR12 polyclonal antibody. Similar to the *FBR12*:*GUS* expression pattern, we detected FBR12 protein in the stele of mature zone of the root and in an extended domain in the elongation zone (Figure 2C). The relatively specific expression pattern of *FBR12* in the root is consistent with the *fbr12* mutant

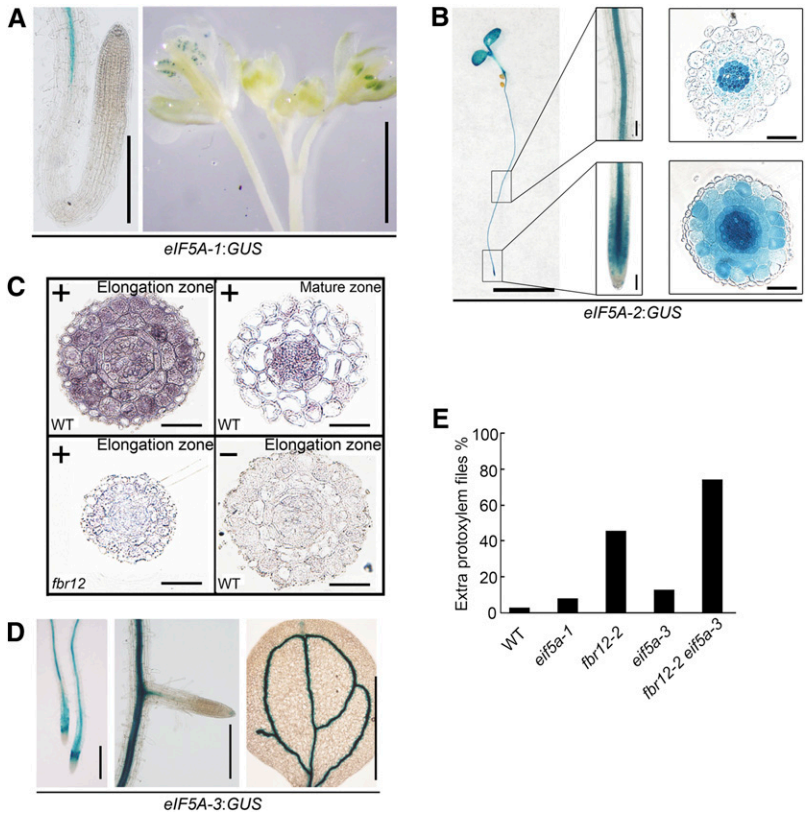

Figure 2. Characterization of *Arabidopsis eIF5A* Genes.

(A) Analysis of *eIF5A-1*:*GUS* expression. Bars = 0.5 cm.
(B) Analysis of *eIF5A-2*/*FBR12*:*GUS* expression. Left, a 4-d-old seedling. Middle, enlarged views of the highlighted region at the left. Right, transverse sections of the matured zone **(top)** and the elongation zone **(bottom)** of the highlighted region shown in the middle. Bars = 5 mm (left), 60 μm (middle), and 20 μm (right).
(C) Immunodetection of FBR12 protein using an anti-FBR12 antibody in transverse sections of the roots derived from 4-d-old seedlings. + and −, with or without an anti-FBR12 antibody, respectively. WT, wild type. Bars = 20 μm.
(D) Analysis of *eIF5A-3*:*GUS* expression. The middle of the panel shows a primary root and the adjacent lateral root. Bars = 0.5 cm.
(E) Analysis of protoxylem development in the *eif5a* mutants ($n > 35$).
Various staining times were used in the GUS reporter assay due to different expression levels of these three *eIF5A* genes. Usually, 6 to 8 h, 5 to 10 min, and 2 to 3 h were used for *eIF5A-1*, *-2*, and *-3*:*GUS* transgenic lines, respectively.

phenotype in root vascular development. *eIF5A-3* expression was substantially lower than that of *FBR12*/*eIF5A-2* (see Supplemental Figures 4A and 4B online), and we detected *eIF5A-3*:*GUS* mainly in the vascular tissues (Figure 2D), suggesting that it may play an important role in vascular development. The *GUS* reporter results were consistent with the microarray data from the *Arabidopsis* electronic fluorescent pictograph browser (Schmid et al., 2005; Winter et al., 2007) (see Supplemental Figure 4A online).

In addition to our characterization of *fbr12* mutants, which affect *eIF5A-2*, we also identified and characterized the *eif5a-1* and *eif5a-3* mutants (see Supplemental Figure 4C online). The expression of *eIF5A-3* was undetectable by quantitative RT-PCR (qRT-PCR) in the *eif5a-3* mutant (see Supplemental Figure 4D online), indicating that the T-DNA insertion causes a null mutation. *eIF5A-1* expression was not detected in both wild-type and *eif5a-1* mutant seedlings by qRT-PCR, presumably owing to its extremely low expression level. Under normal growth conditions, *eif5a-1* and *eif5a-3* showed no apparent abnormalities (see Supplemental Figure 4E online). However, a close examination of root vascular development revealed that both *eif5a-1* and *eif5a-3* had extra protoxylem cell files with a lower phenotypic penetrance than *fbr12-2* (Figure 2E). The *fbr12-2 eif5a-3* double mutant showed a significantly enhanced phenotype (73.9%; Figure 2E), suggesting that these two loci function redundantly in specifying protoxylem development. Because *FBR12*/*eIF5A-2* shows the highest expression level and the *fbr12* mutants display strongest phenotype, we focus on the analysis of *fbr12* hereafter.

Involvement of *FBR12* in Cytokinin Signaling and Cytokinin-Regulated Protoxylem Development

Because defective root protoxylem development in *fbr12* resembles that observed in the cytokinin mutants, we first analyzed the response of *fbr12* roots to exogenous cytokinin.

Treatment with benzyladenine (BA) eliminated protoxylem differentiation in wild-type roots, but protoxylem remained unaltered in *fbr12* roots (Figures 3A and 3B), indicating that cytokinin-regulated protoxylem specification requires *FBR12*.

We next examined the cytokinin response of *fbr12* in several other assays. Cytokinin inhibited primary root growth in wild-type plants, and this inhibitory effect was reduced in *fbr12* (Figure 3C). In a shoot formation assay, *fbr12* explants showed substantially reduced sensitivity to cytokinin compared with wild-type explants (Figure 3D). Moreover, we analyzed the cytokinin-induced expression of all type-A *ARR* genes in wild-type and *fbr12* roots by qRT-PCR. Among the 10 type-A *ARR* genes, expression of most members in *fbr12* roots showed a similar pattern as in wild-type roots (see Supplemental Figure 5 online). However, the cytokinin-induced expression of *ARR15* and *ARR16* was reduced in *fbr12* roots (Figure 3E), suggesting that *FBR12* may specifically regulate the cytokinin-induced expression of *ARR15* and *ARR16*. Notably, whereas *ARR15* and *ARR16* show a reduced expression level in *cre1* (Kiba et al., 2002), *ARR15* has an expanded expression domain in *ahp6* (Mähönen et al., 2006b), suggestive of possible roles of *ARR15* and *ARR16* in *CRE1/AHK4*-mediated root xylem development.

To explore the possible function of *ARR15* and *ARR16*, we identified and characterized *arr15* and *arr16* mutants (see

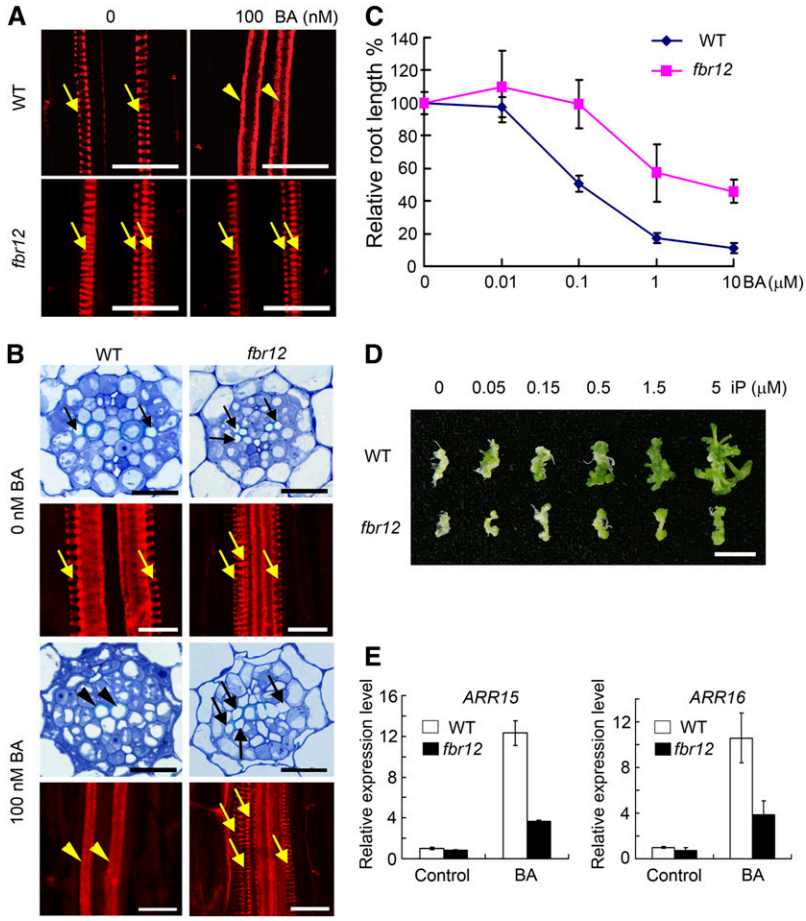

Figure 3. Reduced Cytokinin Sensitivity in *fbr12*.

(A) Cytokinin-regulated protoxylem development at the elongation zone of wild-type (WT) and *fbr12* roots derived from 8-d-old seedlings.

(B) Cytokinin-regulated protoxylem development at the mature zone of wild-type and *fbr12* roots. Eight-day-old seedlings germinated and grown with (100 nM) or without (0 nM) BA were analyzed for the protoxylem cell files.

In **(A)** and **(B)**, arrows and arrowheads indicate protoxylem and metaxylem, respectively. Bars = 20 μm.

(C) The primary root length of wild-type and *fbr12* seedlings germinated and grown on one-half-strength Murashige and Skoog medium containing various concentrations of BA as indicated. The root length in the absence of BA was set as 100% for each genotype. The means of three independent experiments (n = 30) ± SD are shown.

(D) The capacity of shoot formation of wild-type and *fbr12* hypocotyl explants. Hypocotyl explants derived from 4-d-old seedlings were used for the shoot regeneration assay. Representative calli or shoots were photographed after cultured for 3 weeks on the regeneration medium. At least 60 explants of each genotype were used in each experiment. The experiment was repeated three times, and similar results were obtained. Bar = 1 cm.

(E) Expression of cytokinin responsive genes *ARR15* and *ARR16* in wild-type and *fbr12* roots. Seedlings were treated with DMSO (control) or 5 μM BA for 30 min. Data presented are mean values of three independent experiments. Error bars denote SD.

Supplemental Figures 6A and 6B online). Whereas the *arr15* and *arr16* single mutants did not have detectable abnormality in root xylem development, the *arr15 arr16* double mutant showed extra protoxylem cell files (see Supplemental Figure 6C online). An *arr15 arr16 fbr12* triple mutant showed a similar phenotype as *fbr12* in protoxylem development (see Supplemental Figure 6C online). The relatively weak phenotype of the *arr15 arr16* double mutant was presumably caused by functional redundancy among type-A *ARR* genes, as an *arr3*,*4*,*5*,*6*,*8*,*9* hextuple mutant and the overexpression of all type-A *ARR* genes did not have detectable effects on root xylem development (To et al., 2004; Ren et al., 2009). Collectively, these results indicate that *FBR12* plays an important role in the regulation of the cytokinin response.

Previous studies showed that VND7 is a key regulator of root xylem development (Kubo et al., 2005; Yamaguchi et al., 2011). We found that neither the expression level nor the expression domain of VND7 was affected by the *fbr12* mutation (see Supplemental Figures 7A and 7B online). PIN-modulated polar auxin transport plays an important role in the regulation of protoxylem differentiation, in which PIN1, PIN3, and PIN7 play a major role (Bishopp et al., 2011b). We found that the expression domains and the expression levels of PIN1-GFP (for green fluorescent protein), PIN3-GFP, and PIN7-GFP remained largely unaltered in the *fbr12* root compared with that of the wild type (see Supplemental Figures 8A and 8B online). In addition, the expression pattern and the expression level of *DR5*:*GUS*, a reporter gene used for monitoring auxin distribution (Ulmasov et al., 1997), was not altered by the *fbr12* mutation (see Supplemental Figure 8C online). The expression level and the expression pattern of *IAA2*:*GUS*, a reporter gene of auxin signaling, in the *fbr12* root were similar to that in the wild type (see Supplemental Figure 8D online). Auxin is also known to induce the expression of *AHP6* to regulate protoxylem specification (Bishopp et al., 2011b). We found that the *fbr12* mutation did not affect the ability of auxin to induce *AHP6* expression (see Supplemental Figure 8E online). These results suggest that auxin may not be directly involved in the regulation of *FBR12*-modulated root protoxylem development. However, we cannot exclude the possibility that auxin affects other developmental processes mediated by *FBR12*.

FBR12 Genetically Interacts with the Cytokinin Receptor Gene *CRE1*/*WOL*/*AHK4* and *AHP* Genes

The data presented above indicate that *fbr12* shows reduced sensitivity to cytokinin, and we reasoned that *FBR12* might genetically interact with key components in the cytokinin signaling pathway. To test this possibility, we performed a double-mutant analysis (Figures 4A and 4B). The cytokinin receptor mutant *cre1-2* has no apparent abnormalities, including the primary root length (Inoue et al., 2001). However, the cell number inside the stele was slightly reduced, and extra protoxylem cell files were observed in *cre1-2* roots (46.3%, $n = 41$; Figures 4C to 4E). A similar phenotype was also observed in an additional mutant allele, *cre1-13* (see Supplemental Figures 9A to 9C online), suggesting that mutations in *CRE1* cause abnormal development of protoxylem. The *cre1-2 fbr12* double mutant displayed a phenotype similar to *fbr12* in the primary root length and the cell number inside the stele (Figures 4A to 4D). However, the *cre1-2 fbr12* double mutant showed increased penetrance of the extra protoxylem phenotype. Compared with its parents, *fbr12* (44.7%) and *cre1-2* (46.3%), the double mutant (78.0%) had significantly higher percentage of extra protoxylem cell files (Figure 4E). In the most severe case, nearly half of cells inside the stele were transformed into protoxylem cells in the *cre1-2 fbr12* double mutant (Figure 4F). These results indicate that *cre1-2* and *fbr12* enhance the penetrance and the severity of the mutant phenotype during protoxylem development.

To confirm the genetic interaction between these loci, we further analyzed the *wol fbr12* double mutant. The *wol* mutant carries a point mutation in the hormone-binding domain, rendering it incapable of binding cytokinin, and thus exerts a dominant-negative effect, resembling the phenotype of *ahk2 ahk3 cre1/ahk4* triple mutants (Mähönen et al., 2000, 2006a, 2006b). The *wol fbr12* double mutant displayed a phenotype stronger than both *fbr12* and *wol*, including shorter primary roots, fewer cells inside the stele, and the transformation of all stele cells into protoxylem cells (Figures 4A to 4D). Note that, because a *cre1-12 ahk2-2tk ahk3-3* triple mutant displayed a stronger phenotype than the *wol* mutant allele (Mähönen et al., 2006a), *FBR12* may also genetically interact with *AHK2* and *AHK3*. Together, these results indicate that *FBR12* genetically interacts with *CRE1/WOL/AHK4* to regulate protoxylem development.

We next examined possible genetic interactions between *FBR12* and *AHPs*. Whereas mutations in single *AHP* genes do not have apparent phenotype, different combinations of *ahp* mutants show a variety of abnormalities (Hutchison et al., 2006). Among these, the *ahp2*,*3*,*5* triple mutant or multiple mutants containing *ahp2*, *ahp3*, and *ahp5* showed defects in primary root growth and root xylem development (Hutchison et al., 2006). We therefore generated and analyzed an *ahp2*,*3*,*5 fbr12* quadruple mutant. The *ahp2*,*3*,*5 fbr12* mutant had shorter primary roots compared with *fbr12* and *ahp2*,*3*,*5* (Figures 4G and 4H). In xylem development, the *ahp2*,*3*,*5 fbr12* mutant showed an *ahp1*,*2*,*3*,*5*-like phenotype with the increased number of protoxylem cells (Figure 4I). These results suggest that *FBR12* genetically interacts with *AHPs* to regulate root protoxylem development.

FBR12 Physically Interacts with CRE1 and AHP1

The cytokinin receptors mainly localize to the endoplasmic reticulum (Caesar et al., 2011; Wulfetange et al., 2011), and AHP1-5 proteins are distributed in the cytoplasm and the nucleus (Punwani et al., 2010; Feng et al., 2013). An immunostaining experiment using a polyclonal anti-FBR12 antibody revealed that FBR12 localized in the cytoplasm and the nucleus and was more abundant in the cytoplasm (see Supplemental Figure 10 online). Together with the observation that *fbr12* enhances the *cre1*, *wol*, and *ahp2*,*3*,*5* phenotype, the similar subcellular localization of these protein implies that FBR12 may function in a protein complex containing CRE1 and AHP. To test this possibility, we examined whether FBR12 physically interacted CRE1 or AHP proteins. In a protein pull-down assay, His-FBR12 recombinant protein was readily precipitated by glutathione *S*-transferase (GST)-AHP1, but barely by GST-AHP2 and GST-

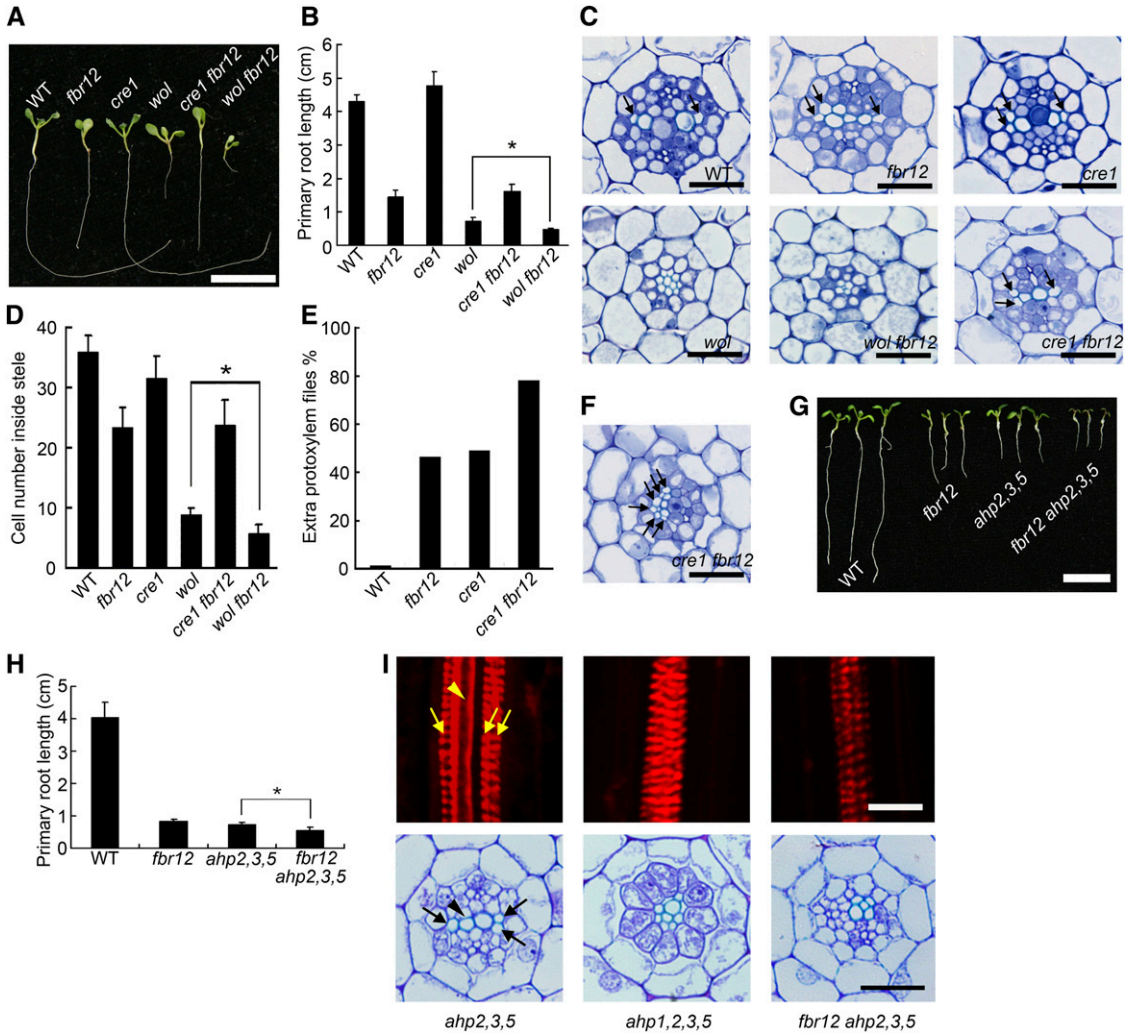

Figure 4. *FBR12* Genetically Interacts with *CRE1/WOL* and *AHP*s.

(A) Eight-day-old seedlings of the wild type (WT) and different mutants with the indicated genotypes. Bar = 1 cm.
(B) Quantitative analysis of the primary root length of wild-type and mutant seedlings shown in **(A)**. Data presented are means ± SD obtained from three independent experiments (n = 30).
(C) Transverse sections of wild-type and mutant roots at the mature zone. Bars = 20 μm.
(D) The cell number inside the stele of wild-type and mutant roots. Data presented were obtained from the analysis of transverse sections of the mature zone of roots (n = 24).
(E) The penetrance of the extra protoxylem phenotype in wild-type and mutant roots with the indicated genotypes (n > 35).
(F) Transverse sections of *cre1-2 fbr12* roots derived from an 8-d-old seedling. Bar = 20 μm.
(G) Eight-day-old seedlings of the wild type and mutants with the indicated genotypes. Bar = 5 mm.
(H) The primary root length of the wild type and mutants with the indicated genotypes shown in **(G)**. Data presented are means ± SD obtained from three independent experiments (n = 30).
(I) *FBR12* and *AHP*s genetically interact to regulate root protoxylem development. **(Top)** Roots derived from 8-d-old seedlings were stained with basic Fuchsin red and analyzed by confocal microscopy (n > 30). **(Bottom)** The transverse sections of roots of 8-d-old seedlings. Bar = 10 μm.
The *cre1-2* allele was used in all experiments. In **(C)**, **(F)**, and **(I)**, yellow arrows and arrowheads indicate protoxylem and metaxylem, respectively. Asterisks in **(B)**, **(D)**, and **(H)** indicate statistically significant difference (analysis of variance, $P < 0.01$).

AHP5 recombinant proteins (Figure 5A). In a reverse reaction, His-FBR12 recombinant protein efficiently pulled down GST-AHP1 and pulled down GST-AHP2 and GST-AHP5 with weaker affinities (Figure 5A). In a firefly luciferase complementation imaging assay (Chen et al., 2008), the physical interaction between FBR12 and AHP1 was specifically detected when transiently expressed in tobacco (*Nicotiana tabacum*) leaves (Figure 5B).

We next explored the possible interactions among CRE1, AHP1, and FBR12 in planta. To this end, we generated antibodies against FBR12, CRE1, and AHP1, which specifically

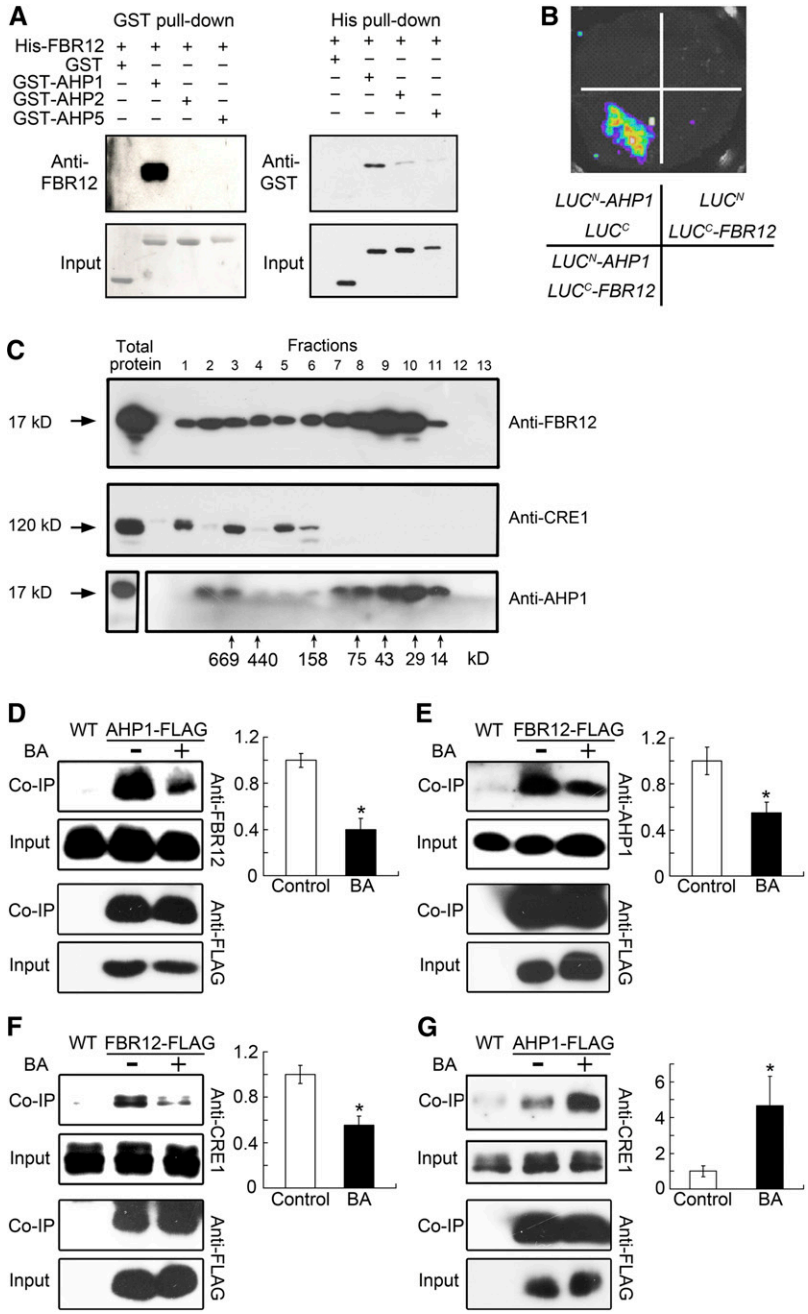

Figure 5. FBR12, CRE1, and AHP1 Compose a Cytokinin-Regulated Complex.

(A) Analysis of the interaction between FBR12 and AHP1 by the protein pull-down assay. The GST- or His-resin–retained proteins were analyzed by immunoblotting using an anti-FBR12 antibody (left) or an anti-GST (right) antibody. Input was examined by Coomassie blue staining.

(B) Analysis of the interaction between FBR12 and AHP1 by luciferase complementation imaging assay. The data shown are representative of three independent experiments.

(C) Gel filtration chromatography of the protein extracts prepared from wild-type roots. Eluted fractions (indicated on the top of the panel) were collected and analyzed by immunoblotting using specific antibodies shown at the right side of the panel. The experiment was repeated three times, and representative results are shown. The approximate molecular mass of the eluted fractionations is shown at the bottom.

(D) through **(G)** Analysis of the interactions among FBR12, CRE1, and AHP1 by coimmunoprecipitation. The protein extracts were prepared from the roots of 3-week-old seedlings treated with (+) or without (−) 5 μM BA for 30 min and then immunoprecipitated with an anti-FLAG antibody. The precipitated samples were analyzed by immunoblotting using the appropriate antibodies as indicated at the right side of the blots. Two independent transgenic lines were analyzed in each experiment. At the right side of each panel, quantitative analysis of the relative level of the coimmunoprecipitation

recognized the target proteins with minimal cross reactivity (see Supplemental Figures 1, 9B, and 11A online) (Feng et al., 2013). We also generated transgenic plants carrying *FBR12*:*FBR12-FLAG* and *AHP1*:*AHP1-FLAG* transgenes, which fully rescued the *fbr12* and *ahp1*,*2*,*3*,*4*,*5* mutant phenotype, respectively (see Supplemental Figures 3 and 11B online). In a gel filtration chromatographic experiment, FBR12, CRE1, and AHP1 proteins eluted in fractions with molecular mass higher than their actual sizes, and their fractionation profiles partially overlapped in the absence or the presence of cytokinin (Figure 5C; see Supplemental Figure 12 online). In particular, all three proteins coeluted in fraction #3, with an approximate molecular mass of 660 kD (Figure 5C), suggesting that these proteins are potentially present in a same protein complex. Moreover, FBR12 and AHP1 also coeluted in fractions #8 through #10, with approximate molecular masses of 29 to 75 kD, which were significantly larger than the expected size of these two proteins (~17 kD; Figure 5C), suggesting that FBR12 and AHP1 may form homooligomers or be present in a complex in the absence of CRE1 or form complexes with other unknown proteins. The fractionation profiles of CRE1 and AHP1 reproducibly displayed a discontinuous pattern, and the reason for this pattern remains to be resolved.

In a coimmunoprecipitation assay, FBR12 was efficiently precipitated using an anti-FLAG antibody in protein extracts from *AHP1-FLAG* transgenic plants (Figure 5D). Conversely, AHP1 was also precipitated in protein extracts from *FBR12-FLAG* transgenic plants with an anti-FLAG antibody (Figure 5E). In both cases, CRE1 was detected with an anti-CRE1 antibody in the anti-FLAG–immunoprecipitated complexes derived from the *AHP1-FLAG* or the *FBR12-FLAG* transgenic plants (Figures 5F and 5G). Notably, the treatment with RNaseA did not have detectable effects on the stability of the FBR12-CRE1-AHP1 complex (see Supplemental Figure 13 online), thus ruling out the possibility that the interaction of FBR12 with CRE1 and AHP1 is RNA dependent. Taken together, these results demonstrate that FBR12, CRE1, and AHP1 occur in a complex in planta.

The *fbr12* mutation did not have detectable effects on the CRE1-AHP1 interaction and subcellular localization of CRE1-GFP and AHP1-GFP (see Supplemental Figures 14 to 16 online). However, treatment with cytokinin reduced the interactions of FBR12-CRE1 and FBR12-AHP1 but enhanced the interaction of AHP1-CRE1 (Figures 5D to 5G). This result suggests that cytokinin regulates the formation of the CRE1-AHP1-FBR12 complex.

Ectopic Expression of *FBR12* in the *CRE1*-Expressing Domain Partially Rescues the *fbr12* Mutant Phenotype

Given that *FBR12* genetically interacts with *CRE1* and *AHP*s and that FBR12 protein forms a complex with CRE1 and AHP1, it is reasonable to assume that these interactions play an important role in the regulation of protoxylem specification. To test this hypothesis, we placed *FBR12* under the control of the *CRE1* promoter and then transformed the *CRE1*:*FBR12* transgene into *fbr12*/+ heterozygous plants (*fbr12*/− homozygous plants are seedling lethal; Feng et al., 2007). We then identified T3 transgenic plants in the wild-type (*fbr12*/+ or *FBR12*/+) or *fbr12*/− mutant background for further analysis.

In the *CRE1*:*FBR12* transgenic plants, *FBR12* was mainly expressed in roots at a level comparable with that of *CRE1* (Figure 6A). We found that the *CRE1*:*FBR12* transgene did not rescue most developmental defects of *fbr12*, including the seedling-lethal phenotype (Figure 6B). Because *CRE1* is mainly expressed in the root (Higuchi et al., 2004; Nishimura et al., 2004), whereas *FBR12* is ubiquitously expressed in most tissues/organs (Feng et al., 2007), it is expected that the *CRE1*:*FBR12* transgene was unable to rescue the *fbr12* mutant phenotype. However, the *CRE1*:*FBR12* transgene partially rescued the defects in protoxylem specification of *fbr12*, by reducing the penetrance of the extra protoxylem phenotype from 46.9 to ~12.5% (four independent transgenic lines were analyzed) in the transgenic lines (Figure 6C). Notably, the *CRE1*:*FBR12* transgene did not restore the primary root length of the transgenic seedlings to that of the wild type (Figure 6D), suggesting that *FBR12* plays a relatively specific role in cytokinin-regulated protoxylem specification.

The *fbr12* Mutant Phenotype Is Partially Suppressed by *ahp6*

The pseudophosphotransfer protein AHP6, a negative regulator of cytokinin signaling, plays a critical role in root protoxylem specification (Mähönen et al., 2006b; Bishopp et al., 2011b). Because *CRE1* genetically interacts with *AHP6* (Mähönen et al., 2006b) and *FBR12*, we then asked whether *AHP6* also genetically interacted with *FBR12* to regulate protoxylem differentiation. To this end, we constructed and analyzed an *ahp6 fbr12* double mutant. The primary root of the *ahp6 fbr12* double mutant was longer than *fbr12* but shorter than *ahp6* (Figures 7A and 7B), indicating that *ahp6* partially suppresses the *fbr12* mutant phenotype. Compared with *fbr12*, the *ahp6 fbr12* double mutant also had an increased cell number inside the stele (Figure 7C). Moreover, the extra protoxylem cell file in the *fbr12* roots (41.5%) was significantly reduced in the *ahp6 fbr12* double mutant (5.6%) (Figures 7D and 7E). However, the incomplete protoxylem cell file remained nearly unaltered in the *fbr12 ahp6* double mutant compared with that in *ahp6* (Figure 7F), indicating that the *fbr12* mutation does not rescue the *ahp6* phenotype. These results suggest that the *ahp6* mutation specifically suppresses the *fbr12* mutant phenotype in protoxylem development.

FBR12 Negatively Regulates the Expression of *AHP6*

The observation that *fbr12* displays a phenotype opposite to that of *ahp6* and that *FBR12* genetically acts upstream of *AHP6* implies that *FBR12* might negatively regulate *AHP6*. To test this

Figure 5. (continued).

samples (the means of four independent experiments ± SD) are shown. Asterisks indicate statistically significant differences compared with control (analysis of variance, $P < 0.01$). WT, wild type.

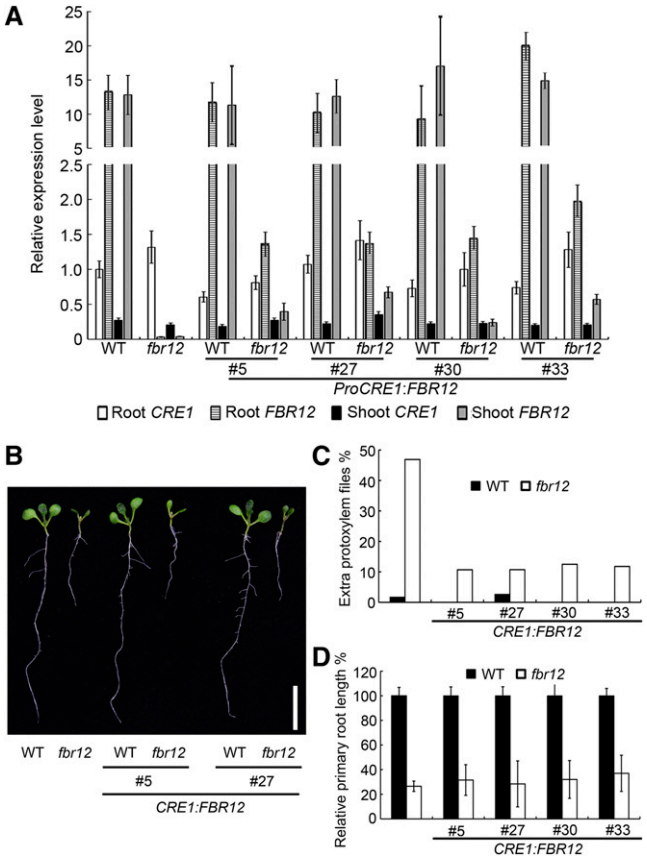

Figure 6. A *CRE1*:*FBR12* Transgene Partially Rescues the *fbr12* Phenotype in Root Protoxylem Development.

(A) Expression of *CRE1* and *FBR12* in wild-type (WT), *fbr12*, and *CRE1*:*FBR12* transgenic seedlings. Total RNA was prepared from roots and shoots of the indicated genotypes and then used for qRT-PCR. In the transgenic samples, wild-type- and *fbr12*-like segregants were derived from self-pollinated *fbr12*/+ plants homozygous for the *CRE1*:*FBR12* transgene. Numbers refer to the transgenic lines. The expression level of *CRE1* in wild-type roots was set as 1.0. The means of three replicates ± SD are shown.

(B) Eight-day-old seedlings of the wild type and the *fbr12* mutants with or without a *CRE1*:*FBR12* transgene. Bar = 1 cm.

(C) Analysis of the extra protoxylem phenotype in the roots of 8-d-old seedlings with the indicated genotypes ($n > 35$).

(D) The relative length of the primary roots of 8-d-old seedlings with the indicated genotypes. For each genotype, the primary root length in the wild-type background was set as 100% ($n = 30$). The means of three replicates ± SD are shown.

possibility, we analyzed *AHP6* expression in *fbr12* roots. A qRT-PCR analysis revealed that the *AHP6* expression was approximately threefold higher in *fbr12* than in the wild type (Figure 8A). The expression level of *AHP1* through *AHP5* in *fbr12* was similar to that in the wild type (see Supplemental Figure 17 online), indicating that the *FBR12*-repressed expression is specific to *AHP6*. Moreover, the expression level and the expression domain of an *AHP6*:*GFP* reporter (Mähönen et al., 2006b) were substantially increased in *fbr12* roots compared with wild-type roots (Figures 8B and 8C). Immunostaining of transverse sections of the *AHP6*:*GFP* roots also revealed that the *AHP6* expression domain expanded (Figure 8D), similar to *cre1 akh3* double mutants (Mähönen et al., 2006b). The expanded expression domain of *AHP6* paralleled the formation of extra protoxylem cells in the *fbr12* root. These results suggest that *FBR12* specifically represses *AHP6* expression.

Cytokinin also represses *AHP6* expression (Mähönen et al., 2006b; Bishopp et al., 2011b). However, the cytokinin repression of *AHP6* expression was remarkably alleviated in the *fbr12* root (Figures 8A and 8B). Intriguingly, *AHP6* expression was detectable in the *fbr12* root treated with a relatively high concentration of cytokinin (500 nM BA) but was completely repressed by a lower concentration of cytokinin (100 nM BA) in wild-type roots (Figure 8B). eIF5A proteins regulate RNA stability (Bevec and Hauber, 1997; Zuk and Jacobson, 1998; Rosorius et al., 1999; Schrader et al., 2006); therefore, it is possible that the reduced *AHP6* mRNA level was caused by its reduced stability mediated by *FBR12*. Compared with *AHP1* mRNA (half-life [*t*1/2] = 109 min in the wild type), *AHP6* mRNA was relatively short-lived with an approximate half-life of 55 min. However, the turnover rate of *AHP6* mRNA was comparable in wild-type and *fbr12* seedlings (see Supplemental Figure 18 online), thus ruling out the possibility that *FBR12* directly regulates *AHP6* mRNA stability. These results suggest that *FBR12* negatively regulates expression of *AHP6* and that cytokinin-repressed expression of *AHP6* depends, at least partly, on *FBR12*.

Overexpression of *AHP6* Mimics the *fbr12* Mutant Phenotype in Protoxylem Specification

The data presented above indicate that *FBR12* negatively regulates *AHP6* expression. In particular, the observation that *ahp6* partially suppresses the *fbr12* mutant phenotype implies that derepression of *AHP6* expression by *fbr12* might cause the misspecification of protoxylem cell files in *fbr12* roots. To test this possibility, we generated transgenic plants overexpressing *AHP6* by the transformation of a 35S:*AHP6* transgene into *FBR12*/*fbr12* heterozygous plants. The wild-type and *fbr12* transgenic segregants were identified and analyzed.

We identified multiple transgenic lines with different increases in *AHP6* transgene expression levels (Figure 8E). Under normal growth conditions, the 35S:*AHP6* transgenic seedlings did not show apparent abnormalities (see Supplemental Figure 19A online). When treated with cytokinin, these 35S:*AHP6* plants showed a similar response as wild-type plants in a root elongation assay (see Supplemental Figure 19B online). However, the cytokinin-induced expression of *ARR15* and *ARR16*, but not that of *ARR7*, was reduced in the roots of the 35S:*AHP6* transgenic plants (Figure 8F), a phenotype similar to that observed in *fbr12* roots (Figure 3E).

Similar to the *fbr12* mutant, all the examined 35S:*AHP6* transgenic plants had extra protoxylem in roots, ranging from 23.1 to 52.9% (Figures 8G and 8H). In the *fbr12* mutant background, the overexpression of *AHP6* substantially increased the phenotypic penetrance of the extra protoxylem compared with that in the wild-type background (Figures 8H and 8I), suggestive

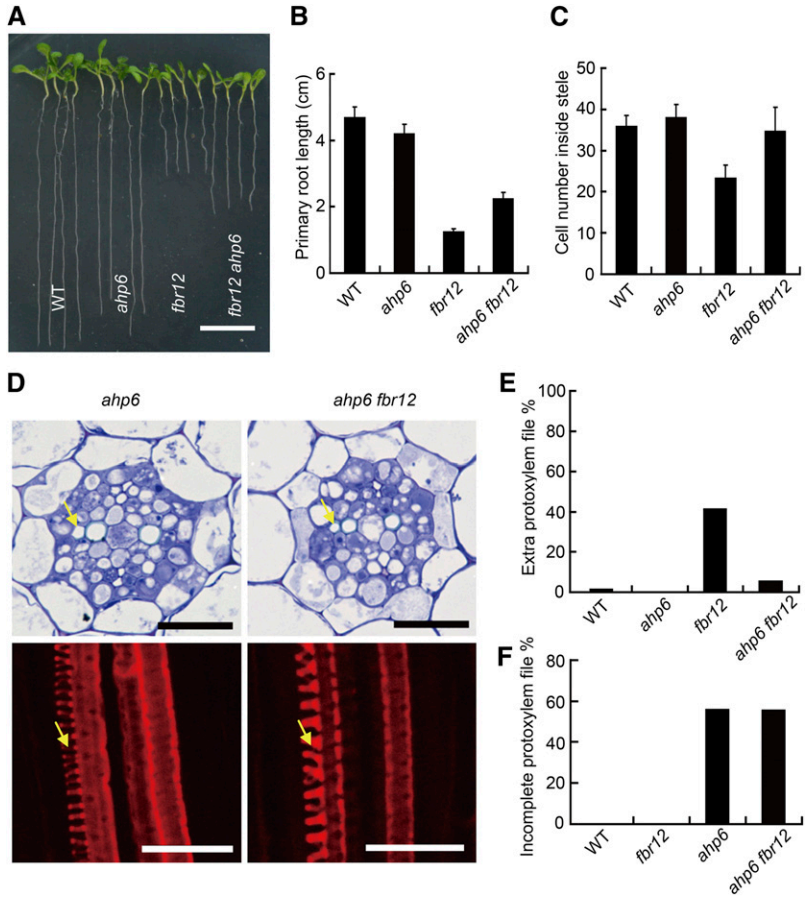

Figure 7. *ahp6* Partially Suppresses the *fbr12* Mutant Phenotype.

(A) Eight-day-old seedlings of the wild type (WT) and mutants with the indicated genotypes. Bar = 1 cm.

(B) Analysis of the primary root length of wild-type and mutant seedlings shown in **(A)**. Data presented are mean values from three independent experiments (n = 30).

(C) The cell number inside the stele. Data presented were obtained from the analysis of transverse sections of the mature zone of the root (n = 30).

(D) Protoxylem development in the *ahp6 fbr12* double mutant. Note that *fbr12* shows a phenotype of extra protoxylem (see Figures 1D, 3A, and 3B), and this phenotype is partially suppressed by the *ahp6* mutation. Bars = 20 μm.

(E) and **(F)** Quantitative analysis of the extra protoxylem cell file **(E)** and the incomplete protoxylem file **(F)** in the roots of the wild type and mutants with the indicated genotypes (n = 36).

of the additive effect of *fbr12* and the overexpression of *AHP6* during root protoxylem development.

DISCUSSION

In this study, we present genetic, cell biology, and biochemical studies demonstrating that FBR12/eIF5A-2 is involved in cytokinin signaling to directly regulate root protoxylem specification. First, root vascular development in *fbr12* is similar to that of cytokinin mutants *cre1*, *wol*, *ahp1*,*2*,*3*,*4*,*5*, and *arr1*,*10*,*12*, characteristic of the formation of extra protoxylem cell files, indicating that *FBR12* is involved in xylem development. In agreement with this view, FBR12 preferentially accumulates in root vascular tissues. Second, *FBR12* genetically interacts with *CRE1/WOL* and *AHP2*,*3*,*5*, suggesting an important role of *FBR12* in cytokinin signaling. The genetic interactions of *FBR12* with the cytokinin signaling components are best shown by their synergistic effects on cell division and cell differentiation in root vascular development. Intriguingly, ectopic expression of *FBR12* in the *CRE1*-expressing domain partially rescues the *fbr12* mutant phenotype in protoxylem development. This result mirrors a previous observation that the depletion of cytokinin in the *CRE1*-expressing domain transform all cell files of the root vascular cylinder into protoxylem (Mähönen et al., 2006b), suggesting that *FBR12* is specifically involved in the cytokinin-regulated protoxylem development. Third, *fbr12* showed substantially reduced sensitivity to cytokinin, including primary root growth, root protoxylem differentiation, and shoot regeneration in vitro as well as the altered expression of *ARR15*, *ARR16*, and *AHP6* in response to cytokinin. Fourth, FBR12 physically interacts with CRE1 and AHP1 in an RNase-insensitive manner, implying a regulatory role of the complex in cytokinin signaling,

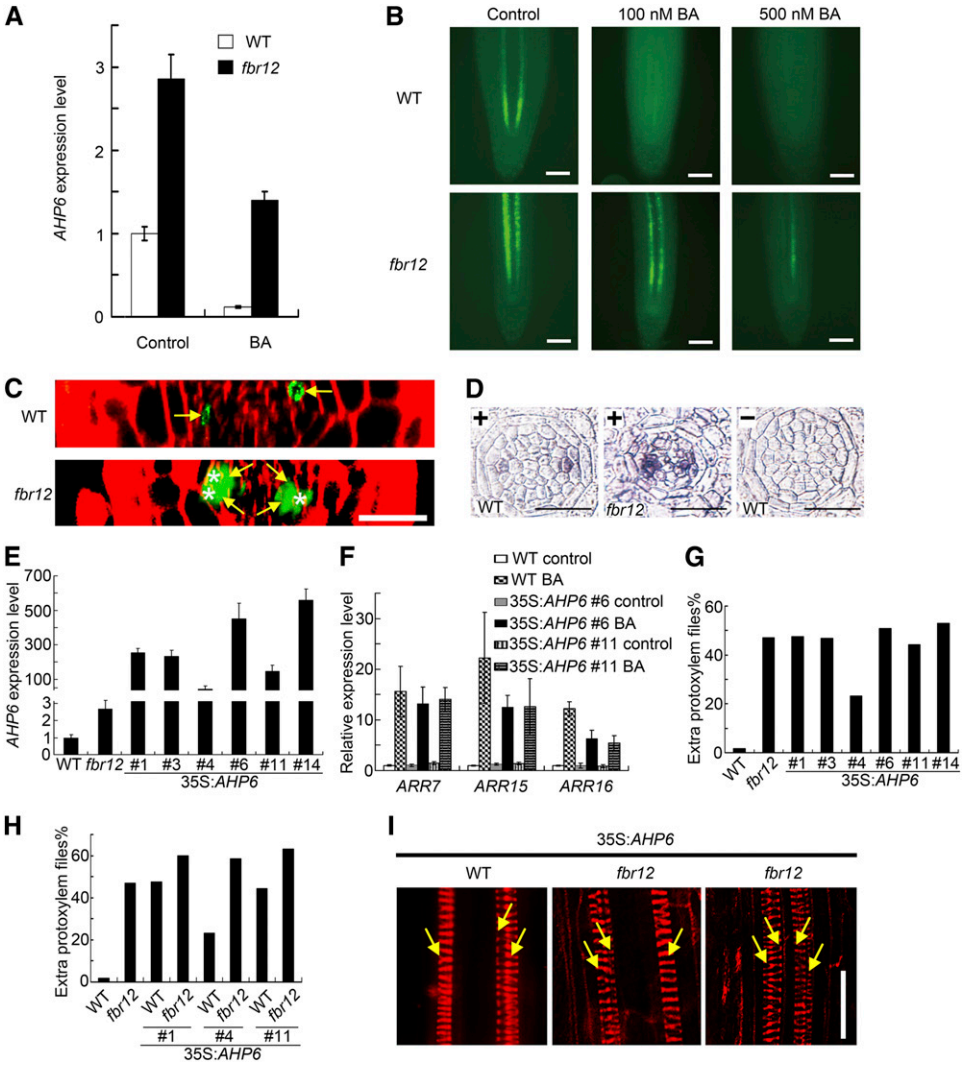

Figure 8. *FBR12* Negatively Regulates the Expression of *AHP6*.

(A) Expression of *AHP6* in wild-type (WT) and *fbr12* roots. Total RNA was prepared from the root derived from 8-d-old seedlings treated with or without 100 nM BA for 3 h and analyzed by qRT-PCR. The means of three replicates ± SD are shown.

(B) Analysis of expression of the *AHP6*:*GFP* reporter gene in wild-type and *fbr12* roots by confocal microscopy. The samples were treated with or without (control) BA for 12 h. Bars = 20 μm.

(C) Confocal sections of *AHP6*:*GFP* in wild-type and *fbr12* roots. The transverse images were reconstructed by collection of Z stacks scanning. Arrows and asterisks denote protoxylem and the protoxylem-adjacent pericycle cells, respectively. Bar = 20 μm.

(D) Immunodetection of *AHP6*:*GFP* expression using an anti-GFP antibody in transverse sections prepared from the root tip derived from 4-d-old wild-type and *fbr12* seedlings. + and −, preparations incubated with and without an anti-GFP antibody, respectively. Bars = 20 μm.

(E) Analysis of *AHP6* expression in 8-d-old 35S:*AHP6* transgenic seedlings by qRT-PCR. The relative expression level in the wild type was set as 1.0. The means of three replicates ± SD are shown.

(F) Analysis of expression of type-A *ARR*s in 35S:*AHP6* transgenic plants. Eight-day-old seedlings were treated with or without 100 nM BA for 30 min. Total RNA was prepared from the roots and then used for qRT-PCR. For each target gene, the relative expression level in untreated wild type was set as 1.0. The means of three replicates ± SD are shown.

(G) Analysis of protoxylem development in the root of 35S:*AHP6* seedlings (8 d old). The sample was stained with basic Fuchsin red, and the xylem phenotype was analyzed and scored under a confocal microscope ($n > 50$).

(H) Quantitative analysis of the extra protoxylem in the root of 8-d-old seedlings with the indicated genotypes ($n > 50$). All 35S:*AHP6* transgenic seedlings were segregants derived from self-pollinated *fbr12*/+ plants homozygous for the 35S:*AHP6* transgene, showing a wild-type-like or *fbr12* phenotype. Numbers refer to transgenic lines.

(I) Confocal scanning microscopy of root xylem development in 35S:*AHP6* transgenic seedlings as described in **(H)**. Representative images with various defects in protoxylem development are shown. Arrows denote protoxylem. Bar = 20 μm.

which might not be directly involved in protein translation. Lastly, *FBR12* specifically represses expression of *AHP6*, a negative regulator of cytokinin signaling. Taken together, these observations reveal an important role of *FBR12* in regulating cytokinin signaling, in particular in cytokinin-regulated xylem development.

The *fbr12* mutant shows a pleiotropic phenotype with severe defects in growth and development (Feng et al., 2007), raising the possibility that the involvement of *FBR12* in cytokinin-regulated protoxylem development is nonspecific. Although *fbr12* displays a reduced response to cytokinin in nearly all the analyzed phenotypes, cytokinin-induced expression of most type-A *ARR* genes is relatively normal. Remarkably, *ARR15* and *ARR16*, two type-A *ARR* genes implied in CRE1/AHK4-meidated signaling in roots (Kiba et al., 2002; Mähönen et al., 2006b), show the reduced induction by cytokinin in the *fbr12* roots, suggesting that *FBR12* specifically modulates the expression of these two genes, but not other type-A *ARR*s. Similarly, expression of *AHP6*, but not other *AHP* genes, is specifically altered by the *fbr12* mutation, thus disfavoring an argument that the altered expression of these genes is caused by a pleiotropic effect. Intriguingly, the pleiotropic phenotype of *fbr12* is partially suppressed by *ahp6*, demonstrating the specificity of the genetic interaction between these two loci. Moreover, whereas the reciprocal inhibition of auxin and cytokinin plays a critical role in root vascular patterning (Bishopp et al., 2011a, 2011b), *fbr12* shows relatively normal auxin signaling in protoxylem development, further supporting a specific role of *FBR12* in cytokinin-regulated protoxylem specification.

The *fbr12* mutant showed a remarkably reduced response to cytokinin, similar to that of the cytokinin signaling mutants in many aspects. Two models can explain the *FBR12* function in cytokinin signaling. First, because of the enhanced phenotype of *fbr12 cre1*, *fbr12 wol*, and *fbr12 ahp2*,*3*,*5* mutants, *FBR12* may function in a pathway independent from *CRE1-AHP*–mediated signaling. This scenario is similar to the observation made in a previous study, in which *LHW* and *WOL* were proposed to function independently to regulate cell division in the stele (Ohashi-Ito and Bergmann, 2007). Alternatively, FBR12 may function in a complex with CRE1 and AHP proteins. Consistent with this notion, our results demonstrate that FBR12 forms a complex with CRE1 and AHP1 in planta. Notably, FBR12 does not appear to affect the stability, the subcellular localization, and the interaction of CRE1 and AHP1 proteins, and we therefore speculate that FBR12 may regulate the phosphorelay activity. In this regard, FBR12 may be a bifunctional molecule that enhances phosphorelay by stabilizing the CRE1-AHP1 complex and also antagonizes the inhibitory effect of AHP6 on the phosphorelay, thereby positively regulating cytokinin signaling. In support of this notion, the CRE1–AHP1 interaction is enhanced by cytokinin, which, in turn, promotes the release of FBR12 from the CRE1-AHP1-FBR12 complex. It will be of great interest to test this hypothesis upon the development of an in vivo assay for phosphorelay activity and, in a more general sense, to understand the precise biochemical function of FBR12 in regulating of the CRE1-AHP1-FBR12 complex.

The conventional cytokinin-mediated phosphorelay is involved in the sequential transfer of a phosphoryl group from the receptor to downstream AHPs (AHP1 through AHP5) and ARRs (To and Kieber, 2008; Hwang et al., 2012). Whereas this linear pathway is negatively regulated by AHP6, which competitively inhibits phosphotransfer from the kinase domain to the receiver domain of the cytokinin receptors and from AHP1 to ARR1 (Mähönen et al., 2006b), the expression of *AHP6* is promoted by auxin, through which auxin antagonizes the action of cytokinin in root vascular patterning (Bishopp et al., 2011b). The discovery that *FBR12* genetically acts upstream of *AHP6* to repress its expression, possibly in an auxin-independent manner, identifies an additional regulatory mechanism in cytokinin-regulated root protoxylem development. Because an *AHP6*:*GFP* reporter gene shows an increased expression level and an expanded expression domain in the *fbr12* root, *FBR12*-regulated *AHP6* expression may occur mainly at the transcriptional level, but not at the posttranscriptional level such as eIF5A-regulated RNA stability (Zuk and Jacobson, 1998; Valentini et al., 2002). The expression of *AHP6* is negatively regulated by cytokinin at the transcriptional level in a cytokinin receptor–dependent manner (Mähönen et al., 2006b). However, the molecular mechanism of this regulation remains elusive. We speculate that the CRE1-AHP1-FBR12 complex coordinates the input of cytokinin signaling, whereas the cytokinin-repressed expression of *AHP6* represents a major output signal, which, in turn, negatively regulates cytokinin signaling. Presumably, the expression of *AHP6* is regulated by a transcription repressor that can be inactivated by cytokinin through the CRE1-AHP1-FBR12 complex. The identification and characterization of this putative repressor will be a key toward full understanding the molecular mechanism of the cytokinin-regulated protoxylem development.

The evolutionarily conserved eIF-5A proteins have long been proposed to modulate cell division, cell differentiation, and cell death by the regulation of protein translation initiation, RNA turnover, and RNA trafficking, in spite of limited biochemical evidence available for the proposed activities. In *Arabidopsis*, eIF5A proteins, including FBR12, have been associated with diverse physiological and pathological processes, including leaf senescence, fruit ripening, stem xylem development, the stress response, and the hypersensitive response (Wang et al., 2001, 2005; Feng et al., 2007; Hopkins et al., 2008; Liu et al., 2008b; Ma et al., 2010). The *fbr12* mutant was originally identified as an anti–cell-death mutant (Feng et al., 2007), and the discovery made in this study identifies *FBR12*/*eIF5A-2* as a key regulator of root protoxylem development by modulating cytokinin signaling, thus adding a component in the framework of cytokinin signaling and cytokinin-regulated protoxylem development. In summary, the results presented in this study define a specific cellular activity of the highly conserved eIF5A proteins during growth and development of higher plants, which should also provide useful information for functional studies of eIF5A in other eukaryotes.

METHODS

Plant Materials and Growth Conditions

The wild type *Arabidopsis thaliana* Ws and Col-0 accessions were used in this study. The *fbr12* mutant is in the Ws background (Feng et al., 2007),

and all other mutants and transgenic lines are in the Col-0 background. The *fbr12-2*, *ahp1-1*, *cre1-13*, *arr15*, *arr16*, *eif5a-1*, and *eif5a-3* mutant seeds were obtained from the ABRC or GABI-KAT. For the double mutant analysis, the segregated wild-type progenies in F2 or F3 populations were used as controls in all experiments.

Seeds were sterilized and sown on GM medium (one-half-strength Murashige and Skoog salts, 1% Suc, 1× B5 vitamin, 0.05% MES-KOH, and 0.3% Phytagel), stratified in the dark at 4°C for 2 d, and germinated and grown at 22°C under the continuous white light (120 mmol m^{-2} s^{-1}) for appropriate time. The root elongation and the shoot formation assays were performed as described previously (Deng et al., 2010).

Microscopy

To prepare transverse sections of mature roots, approximate 1-cm-long segments in the root hair zone adjacent to the root tip side were hand dissected. The samples were fixed overnight in PBS containing 4% glutaraldehyde and embedded in Leica Historesin. Serial semithin sections (1 μm) were made on a Leica RM6625 rotary microtome, stained by toluidine blue (0.1% [w/v]), and analyzed under a microscope. For each sample, at least two to three sections were analyzed, and sections that contained more than two or less than two protoxylem cells were defined as extra protoxylem or incomplete protoxylem files, respectively. Basic Fuchsin red staining was performed according to Mähönen et al. (2000).

Preparation of Antibodies and Immunoblot Analysis

The anti-AHP1 polyclonal antibody has been previously described (Feng et al., 2013). To prepare anti-FBR12 and anti-CRE1 antibodies, the full-length *FBR12* cDNA fragments and a fragment encoding amino acid residues 749 to 994 of CRE1 were used to produce recombinant proteins tagged with 6X His and GST, respectively. The purified 6X His-tagged recombinant proteins were used to immunize rabbits, and the resulting antisera were affinity purified using the GST-tagged recombinant protein as a ligand. Immunoblotting was performed as described previously (Ren et al., 2009).

Immunostaining and GUS Assay

Immunostaining was performed as described (Sessions et al., 2000) with minor modifications. Blocking and all subsequent reactions were performed in TBST buffer (150 mM NaCl, 20 mM Tris-HCl, pH 8.0, 0.05% [v/v] Tween 20, and 0.3% [v/v] Triton 100) containing 5% nonfat milk. Primary (anti-FBR12) and secondary (goat anti-rabbit IgG-conjugated with alkaline-phosphatase; Pierce Biotechnology) antibodies were diluted 1:100 and 1:200, respectively, in the reactions. The preparations were developed with nitro blue tetrazolium/5-bromo-4-chloro-3-indolyl phosphate for 2 h. The staining without the primary antibody was used as a negative control. Under the assay conditions, no signal was observed in sections of *fbr12* roots.

Whole-mount immunofluorescence staining was performed as described (Sauer et al., 2006). The sample was incubated with the primary (anti-FBR12) and the secondary (Alexa Fluor 585 goat anti-rabbit IgG; Invitrogen) antibodies. Nuclei were stained by 4′,6-diamidino-2-phenylindole. After washing and mounting, the sample was analyzed under an Olympus Fluoview1000 confocal laser scanning microscope.

GUS activity was analyzed as described previously (Jefferson et al., 1987).

Protein Pull-Down Assay

GST- and His-tagged recombinant proteins were prepared and purified in the pGEX (Amersham Pharmacia) and pQE (Qiagen) vectors according to the manufacturers' instructions.

Protein pull-down assay was performed as described (Liu et al., 2008a) with modifications. Briefly, purified GST, GST fusion proteins, and His-FBR12 protein were immobilized on Glutathione Sepharose 4B and 3S-nitrilotriacetic acid resin, respectively. Immobilized Sepharose beads containing 2 μg GST- or His-tagged fusion proteins were mixed with 1 μg His-FBR12 or GST-tagged proteins and then incubated at 4°C for 1 h. After centrifugation at 800 rpm 4°C for 1 min, the supernatant was removed, and the beads were washed six times with precooled washing buffer (25 mM Tris-HCl, pH 8.0, 150 mM NaCl, 0.1% Triton X-100, and 1 mM phenylmethanesulfonyl fluoride). The sample was then analyzed by immunoblotting.

Coimmunoprecipitation Experiments

The coimmunoprecipitation experiment was performed according to Liu et al. (2008a) with modifications. The sample was prepared by grinding root materials (~0.5 g) in liquid nitrogen and immediately extracting with grinding buffer (50 mM Tris, pH 7.5, 150 mM NaCl, 10 mM $MgCl_2$, 10% glycerol, 0.1% Nonidet P-40, 1 mM phenylmethylsulfonyl fluoride, and 1× Protease Inhibitor Cocktail [Sigma-Aldrich]). After preclearing with Protein A-Agarose (Sigma-Aldrich), 1.5 mg of total protein for each sample was incubated with 50 μL of anti-FLAG M2 Affinity Agarose beads (Sigma-Aldrich) at 4°C for 4 h. The pellets were washed with the grinding buffer for six times and then used for immunoblotting.

Gel Filtration Chromatography

Gel filtration chromatography was performed as previously described (Saini et al., 2009; Ma et al., 2010). Total protein prepared from the roots of 3-week-old seedlings was loaded on a Superdex 10/300 GL prepacked Tricorn column (GE Healthcare), and the collected fractions (1 mL per fraction) were analyzed by immunoblotting using anti-AHP1, anti-CRE1, and anti-FBR12 antibodies. The molecular mass standards were a mixture of Gel Filtration LMW calibration kit (17 to 75 kD; GE Healthcare) and Gel Filtration HMW calibration kit (43 to 669 kD; GE Healthcare).

Molecular Manipulations

All molecular cloning was done by standard methods (Sambrook and Russell, 2001). To make *FBR12*:*GUS*, a 0.9-kb genomic fragment containing the putative *FBR12* promoter region and the entire 5′-untranslated region was PCR amplified (see Supplemental Table 1 online for primers used in this study). A similar fragment was used in the genetic complementation experiment (Feng et al., 2007). This fragment was inserted into the *Hin*dIII and *Bam*HI sites of pBI101 (Clontech) to generate the *FBR12*:*GUS* reporter gene, in which the sequence encoding the first seven amino acid residues of FBR12 was in-frame fused to the *GUS* coding sequence. The *FBR12* and *AHP1* genomic sequences containing the promoter and coding regions were PCR amplified, and the stop codons were removed during PCR. The PCR fragments were fused in frame to a 1× FLAG tag and then inserted into a pER8 vector (Zuo et al., 2000). The resulting transgenes fully rescued the *fbr12* and *ahp1*,*2*,*3*,*4*,*5* mutant phenotypes, respectively. An *AHP6* genomic DNA fragment was amplified by PCR and inserted into a pCAMBIA 2300 vector under the control of a cauliflower mosaic virus 35S promoter. The Lys-51–to–Ser-51 mutation was made by a PCR-based method using appropriate primers spanning the mutated site. A *Bam*HI site was introduced in the mutated region, which was used for genotyping of the transgene.

Total RNA was prepared using the RNeasy plant mini kit (Qiagen) and then treated with the RNase-free DNase set (Qiagen) for 15 min at room temperatures. Real-time qRT-PCR was performed as described (Deng et al., 2010). Real-time PCR was performed using the UltraSYBR mixture (CWBIO) according to the manufacturer's instructions, and the reactions were run in a CFX96TM real-time PCR detection system (Bio-Rad).

Accession Numbers

Sequence data from this article can be found in the Arabidopsis Genome Initiative or GenBank/EMBL databases under the following accession numbers: *ACT7* (AT5G09810), *AHP1* (AT3G21510), *AHP2* (AT3G29350), *AHP3* (AT5G39340), *AHP4* (AT3G16360), *AHP5* (AT1G03430), *AHP6* (AT1G80100), *ARR3* (AT1G59940), *ARR4* (AT1G10470), *ARR5* (AT3G48100), *ARR6* (AT5G62920), *ARR7* (AT1G19050), *ARR8* (AT2G41310), *ARR9* (AT3G57040), *ARR15* (AT1G74890), *ARR16* (AT2G40670), *ARR17* (AT3G56380), *CRE1/WOL* (AT2G01830), *eIF5A-1* (AT1G13950), *eIF5A-2/FBR12* (AT1G26630), and *eIF5A-3* (AT1G69410).

Supplemental Data

The following materials are available in the online version of this article.

Supplemental Figure 1. Analysis of FBR12 Protein in Wild-Type and the *fbr12* Mutant Plants.

Supplemental Figure 2. The *fbr12-2* Mutant Phenotype.

Supplemental Figure 3. Rescue of the *fbr12* Mutant by FBR12 Transgenes.

Supplemental Figure 4. Characterization of the *eIF5A* Gene Family.

Supplemental Figure 5. Analysis of the Expressions Level of Type-A *ARR* Genes.

Supplemental Figure 6. Analysis of Protoxylem Development in *arr15* and *arr16* Mutants.

Supplemental Figure 7. Analysis of the Expression level and the Expression Pattern of *VND7* in *fbr12*.

Supplemental Figure 8. *FBR12* May Act Independently from the Auxin Pathway to Regulate Protoxylem Development.

Supplemental Figure 9. Characterization of the *cre1-13* Mutant Allele.

Supplemental Figure 10. Analysis of Subcellular Localization of FBR12 Protein by Immunofluorescence Staining.

Supplemental Figure 11. Characterization of Anti-AHP1 Antibody and the *AHP1:AHP1-FLAG* Transgenic Plants.

Supplemental Figure 12. Gel-Filtration Chromatography of CRE1, AHP1, and FBR12.

Supplemental Figure 13. The Interaction of FBR12 with CRE1 and AHP1 Is RNA Independent.

Supplemental Figure 14. Analysis of the CRE1-AHP1 Interaction in Wild-Type and *fbr12* Plants.

Supplemental Figure 15. Characterization of the *CRE1*:*CRE1-GFP* Transgenic Plants.

Supplemental Figure 16. Characterization of the *AHP1:AHP1-GFP* Transgenic Plants.

Supplemental Figure 17. Analysis of the Expression Level of *AHP* Genes in *fbr12*.

Supplemental Figure 18. Analysis of the RNA Turnover Rate of *AHP6* mRNA.

Supplemental Figure 19. Characterization of the 35S:*AHP6* Transgenic Plants.

Supplemental Table 1. Primers Used in This Study.

ACKNOWLEDGMENTS

We thank the ABRC, the Nottingham Arabidopsis Stock Centre, Tatsuo Kakimoto, Ykä Helariutta, Thomas Schmülling, Joseph Kieber, Shouyi Chen, Jinsong Zhang, Taku Demura, and Jianwei Pan for providing mutant and transgenic seeds. This work was supported by grants from the National Natural Science Foundation (NSFC 90817107 and 91217302) and the State Key Laboratory of Plant Genomics (2011B0525-02).

AUTHOR CONTRIBUTIONS

B.R., Q.C., and J.Z. designed the research, analyzed the results, and wrote the article. B.R. and Q.C. performed the majority of the experiments, assisted by S.H., W.Z., J.F., and H.F.

Received July 16, 2013; revised September 4, 2013; accepted October 6, 2013; published October 25, 2013.

REFERENCES

Argyros, R.D., Mathews, D.E., Chiang, Y.-H., Palmer, C.M., Thibault, D.M., Etheridge, N., Argyros, D.A., Mason, M.G., Kieber, J.J., and Schaller, G.E. (2008). Type B response regulators of *Arabidopsis* play key roles in cytokinin signaling and plant development. Plant Cell **20:** 2102–2116.

Bevec, D., and Hauber, J. (1997). Eukaryotic initiation factor 5A activity and HIV-1 Rev function. Biol. Signals **6:** 124–133.

Bishopp, A., Benková, E., and Helariutta, Y. (2011a). Sending mixed messages: Auxin-cytokinin crosstalk in roots. Curr. Opin. Plant Biol. **14:** 10–16.

Bishopp, A., Help, H., El-Showk, S., Weijers, D., Scheres, B., Friml, J., Benková, E., Mähönen, A.P., and Helariutta, Y. (2011b). A mutually inhibitory interaction between auxin and cytokinin specifies vascular pattern in roots. Curr. Biol. **21:** 917–926.

Caesar, K., Thamm, A.M.K., Witthöft, J., Elgass, K., Huppenberger, P., Grefen, C., Horak, J., and Harter, K. (2011). Evidence for the localization of the *Arabidopsis* cytokinin receptors AHK3 and AHK4 in the endoplasmic reticulum. J. Exp. Bot. **62:** 5571–5580.

Chen, H., Zou, Y., Shang, Y., Lin, H., Wang, Y., Cai, R., Tang, X., and Zhou, J.-M. (2008). Firefly luciferase complementation imaging assay for protein-protein interactions in plants. Plant Physiol. **146:** 368–376.

Deng, Y., Dong, H., Mu, J., Ren, B., Zheng, B., Ji, Z., Yang, W.-C., Liang, Y., and Zuo, J. (2010). *Arabidopsis* histidine kinase CKI1 acts upstream of histidine phosphotransfer proteins to regulate female gametophyte development and vegetative growth. Plant Cell **22:** 1232–1248.

Dolan, L., Janmaat, K., Willemsen, V., Linstead, P., Poethig, S., Roberts, K., and Scheres, B. (1993). Cellular organisation of the *Arabidopsis thaliana* root. Development **119:** 71–84.

Feng, H., Chen, Q., Feng, J., Zhang, J., Yang, X., and Zuo, J. (2007). Functional characterization of the Arabidopsis eukaryotic translation initiation factor 5A-2 that plays a crucial role in plant growth and development by regulating cell division, cell growth, and cell death. Plant Physiol. **144:** 1531–1545.

Feng, J., Wang, C., Chen, Q., Chen, H., Ren, B., Li, X., and Zuo, J. (2013). S-nitrosylation of phosphotransfer proteins represses cytokinin signaling. Nat Commun **4:** 1529.

Fukuda, H. (2004). Signals that control plant vascular cell differentiation. Nat. Rev. Mol. Cell Biol. **5:** 379–391.

Higuchi, M., et al. (2004). *In planta* functions of the *Arabidopsis* cytokinin receptor family. Proc. Natl. Acad. Sci. USA **101:** 8821–8826.

Hofmann, W., Reichart, B., Ewald, A., Müller, E., Schmitt, I., Stauber, R.H., Lottspeich, F., Jockusch, B.M., Scheer, U., Hauber, J., and Dabauvalle, M.C. (2001). Cofactor requirements for

nuclear export of Rev response element (RRE)- and constitutive transport element (CTE)-containing retroviral RNAs. An unexpected role for actin. J. Cell Biol. **152:** 895–910.

Hopkins, M.T., Lampi, Y., Wang, T.-W., Liu, Z., and Thompson, J.E. (2008). Eukaryotic translation initiation factor 5A is involved in pathogen-induced cell death and development of disease symptoms in Arabidopsis. Plant Physiol. **148:** 479–489.

Hutchison, C.E., Li, J., Argueso, C., Gonzalez, M., Lee, E., Lewis, M.W., Maxwell, B.B., Perdue, T.D., Schaller, G.E., Alonso, J.M., Ecker, J.R., and Kieber, J.J. (2006). The *Arabidopsis* histidine phosphotransfer proteins are redundant positive regulators of cytokinin signaling. Plant Cell **18:** 3073–3087.

Hwang, I., and Sheen, J. (2001). Two-component circuitry in *Arabidopsis* cytokinin signal transduction. Nature **413:** 383–389.

Hwang, I., Sheen, J., and Müller, B. (2012). Cytokinin signaling networks. Annu. Rev. Plant Biol. **63:** 353–380.

Inoue, T., Higuchi, M., Hashimoto, Y., Seki, M., Kobayashi, M., Kato, T., Tabata, S., Shinozaki, K., and Kakimoto, T. (2001). Identification of CRE1 as a cytokinin receptor from *Arabidopsis*. Nature **409:** 1060–1063.

Ishida, K., Yamashino, T., Yokoyama, A., and Mizuno, T. (2008). Three type-B response regulators, ARR1, ARR10 and ARR12, play essential but redundant roles in cytokinin signal transduction throughout the life cycle of *Arabidopsis thaliana*. Plant Cell Physiol. **49:** 47–57.

Jao, D.L.-E., and Chen, K.Y. (2006). Tandem affinity purification revealed the hypusine-dependent binding of eukaryotic initiation factor 5A to the translating 80S ribosomal complex. J. Cell. Biochem. **97:** 583–598.

Jefferson, R.A., Kavanagh, T.A., and Bevan, M.W. (1987). GUS fusions: Beta-glucuronidase as a sensitive and versatile gene fusion marker in higher plants. EMBO J. **6:** 3901–3907.

Kang, H.A., and Hershey, J.W. (1994). Effect of initiation factor eIF-5A depletion on protein synthesis and proliferation of *Saccharomyces cerevisiae*. J. Biol. Chem. **269:** 3934–3940.

Kemper, W.M., Berry, K.W., and Merrick, W.C. (1976). Purification and properties of rabbit reticulocyte protein synthesis initiation factors M2Balpha and M2Bbeta. J. Biol. Chem. **251:** 5551–5557.

Kiba, T., Yamada, H., and Mizuno, T. (2002). Characterization of the ARR15 and ARR16 response regulators with special reference to the cytokinin signaling pathway mediated by the AHK4 histidine kinase in roots of *Arabidopsis thaliana*. Plant Cell Physiol. **43:** 1059–1066.

Kim, H.J., Chiang, Y.-H., Kieber, J.J., and Schaller, G.E. (2013). SCF(^{KMD}) controls cytokinin signaling by regulating the degradation of type-B response regulators. Proc. Natl. Acad. Sci. USA **110:** 10028–10033.

Kim, K., Ryu, H., Cho, Y.-H., Scacchi, E., Sabatini, S., and Hwang, I. (2012). Cytokinin-facilitated proteolysis of *ARABIDOPSIS* RESPONSE REGULATOR 2 attenuates signaling output in two-component circuitry. Plant J. **69:** 934–945.

Kubo, M., Udagawa, M., Nishikubo, N., Horiguchi, G., Yamaguchi, M., Ito, J., Mimura, T., Fukuda, H., and Demura, T. (2005). Transcription switches for protoxylem and metaxylem vessel formation. Genes Dev. **19:** 1855–1860.

Li, A.-L., et al. (2004). A novel eIF5A complex functions as a regulator of p53 and p53-dependent apoptosis. J. Biol. Chem. **279:** 49251–49258.

Lipowsky, G., Bischoff, F.R., Schwarzmaier, P., Kraft, R., Kostka, S., Hartmann, E., Kutay, U., and Görlich, D. (2000). Exportin 4: A mediator of a novel nuclear export pathway in higher eukaryotes. EMBO J. **19:** 4362–4371.

Liu, H., Yu, X., Li, K., Klejnot, J., Yang, H., Lisiero, D., and Lin, C. (2008a). Photoexcited CRY2 interacts with CIB1 to regulate transcription and floral initiation in *Arabidopsis*. Science **322:** 1535–1539.

Liu, Z., Duguay, J., Ma, F., Wang, T.-W., Tshin, R., Hopkins, M.T., McNamara, L., and Thompson, J.E. (2008b). Modulation of eIF5A1 expression alters xylem abundance in *Arabidopsis thaliana*. J. Exp. Bot. **59:** 939–950 10.1093/jxb/ern1017.

Mähönen, A.P., Bonke, M., Kauppinen, L., Riikonen, M., Benfey, P.N., and Helariutta, Y. (2000). A novel two-component hybrid molecule regulates vascular morphogenesis of the *Arabidopsis* root. Genes Dev. **14:** 2938–2943.

Mähönen, A.P., Higuchi, M., Törmäkangas, K., Miyawaki, K., Pischke, M.S., Sussman, M.R., Helariutta, Y., and Kakimoto, T. (2006a). Cytokinins regulate a bidirectional phosphorelay network in *Arabidopsis*. Curr. Biol. **16:** 1116–1122.

Mähönen, A.P., Bishopp, A., Higuchi, M., Nieminen, K.M., Kinoshita, K., Törmäkangas, K., Ikeda, Y., Oka, A., Kakimoto, T., and Helariutta, Y. (2006b). Cytokinin signaling and its inhibitor AHP6 regulate cell fate during vascular development. Science **311:** 94–98.

Müller, B., and Sheen, J. (2008). Cytokinin and auxin interaction in root stem-cell specification during early embryogenesis. Nature **453:** 1094–1097.

Ma, Y., Miura, E., Ham, B.-K., Cheng, H.-W., Lee, Y.-J., and Lucas, W.J. (2010). Pumpkin eIF5A isoforms interact with components of the translational machinery in the cucurbit sieve tube system. Plant J. **64:** 536–550.

Nishimura, C., Ohashi, Y., Sato, S., Kato, T., Tabata, S., and Ueguchi, C. (2004). Histidine kinase homologs that act as cytokinin receptors possess overlapping functions in the regulation of shoot and root growth in *Arabidopsis*. Plant Cell **16:** 1365–1377.

Ohashi-Ito, K., and Bergmann, D.C. (2007). Regulation of the *Arabidopsis* root vascular initial population by LONESOME HIGHWAY. Development **134:** 2959–2968.

Park, M.H., Lee, Y.B., and Joe, Y.A. (1997). Hypusine is essential for eukaryotic cell proliferation. Biol. Signals **6:** 115–123.

Punwani, J.A., Hutchison, C.E., Schaller, G.E., and Kieber, J.J. (2010). The subcellular distribution of the *Arabidopsis* histidine phosphotransfer proteins is independent of cytokinin signaling. Plant J. **62:** 473–482.

Ren, B., Liang, Y., Deng, Y., Chen, Q., Zhang, J., Yang, X., and Zuo, J. (2009). Genome-wide comparative analysis of type-A *Arabidopsis response regulator* genes by overexpression studies reveals their diverse roles and regulatory mechanisms in cytokinin signaling. Cell Res. **19:** 1178–1190.

Rosorius, O., Reichart, B., Krätzer, F., Heger, P., Dabauvalle, M.-C., and Hauber, J. (1999). Nuclear pore localization and nucleocytoplasmic transport of eIF-5A: Evidence for direct interaction with the export receptor CRM1. J. Cell Sci. **112:** 2369–2380.

Saini, P., Eyler, D.E., Green, R., and Dever, T.E. (2009). Hypusine-containing protein eIF5A promotes translation elongation. Nature **459:** 118–121.

Sambrook, J., and Russell, D.W. (2001). Molecular Cloning: A Laboratory Manual. (Cold Spring Harbor, NY: Cold Spring Harbor Laboratory Press).

Sauer, M., Paciorek, T., Benková, E., and Friml, J. (2006). Immunocytochemical techniques for whole-mount in situ protein localization in plants. Nat. Protoc. **1:** 98–103.

Schmid, M., Davison, T.S., Henz, S.R., Pape, U.J., Demar, M., Vingron, M., Schölkopf, B., Weigel, D., and Lohmann, J.U. (2005). A gene expression map of *Arabidopsis thaliana* development. Nat. Genet. **37:** 501–506.

Schrader, R., Young, C., Kozian, D., Hoffmann, R., and Lottspeich, F. (2006). Temperature-sensitive eIF5A mutant accumulates transcripts targeted to the nonsense-mediated decay pathway. J. Biol. Chem. **281:** 35336–35346.

Sessions, A., Yanofsky, M.F., and Weigel, D. (2000). Cell-cell signaling and movement by the floral transcription factors LEAFY and APETALA1. Science **289:** 779–782.

Steeves, T.A., and Sussex, I.M. (1989). Patterns in Plant Development. (Cambridge, UK: Cambridge University Press).

Thompson, G.M., Cano, V.S., and Valentini, S.R. (2003). Mapping eIF5A binding sites for Dys1 and Lia1: in vivo evidence for regulation of eIF5A hypusination. FEBS Lett. **555:** 464–468.

Thompson, J.E., Hopkins, M.T., Taylor, C., and Wang, T.W. (2004). Regulation of senescence by eukaryotic translation initiation factor 5A: Implications for plant growth and development. Trends Plant Sci. **9:** 174–179.

To, J.P.C., Haberer, G., Ferreira, F.J., Deruère, J., Mason, M.G., Schaller, G.E., Alonso, J.M., Ecker, J.R., and Kieber, J.J. (2004). Type-A *Arabidopsis* response regulators are partially redundant negative regulators of cytokinin signaling. Plant Cell **16:** 658–671.

To, J.P.C., and Kieber, J.J. (2008). Cytokinin signaling: Two-components and more. Trends Plant Sci. **13:** 85–92.

Ulmasov, T., Murfett, J., Hagen, G., and Guilfoyle, T.J. (1997). Aux/IAA proteins repress expression of reporter genes containing natural and highly active synthetic auxin response elements. Plant Cell **9:** 1963–1971.

Valentini, S.R., Casolari, J.M., Oliveira, C.C., Silver, P.A., and McBride, A.E. (2002). Genetic interactions of yeast eukaryotic translation initiation factor 5A (eIF5A) reveal connections to poly(A)-binding protein and protein kinase C signaling. Genetics **160:** 393–405.

Wang, T.-W., Lu, L., Wang, D., and Thompson, J.E. (2001). Isolation and characterization of senescence-induced cDNAs encoding deoxyhypusine synthase and eucaryotic translation initiation factor 5A from tomato. J. Biol. Chem. **276:** 17541–17549.

Wang, T.-W., Zhang, C.-G., Wu, W., Nowack, L.M., Madey, E., and Thompson, J.E. (2005). Antisense suppression of deoxyhypusine synthase in tomato delays fruit softening and alters growth and development. Plant Physiol. **138:** 1372–1382.

Werner, T., and Schmülling, T. (2009). Cytokinin action in plant development. Curr. Opin. Plant Biol. **12:** 527–538.

Winter, D., Vinegar, B., Nahal, H., Ammar, R., Wilson, G.V., and Provart, N.J. (2007). An "Electronic Fluorescent Pictograph" browser for exploring and analyzing large-scale biological data sets. PLoS ONE **2:** e718.

Wulfetange, K., Lomin, S.N., Romanov, G.A., Stolz, A., Heyl, A., and Schmülling, T. (2011). The cytokinin receptors of Arabidopsis are located mainly to the endoplasmic reticulum. Plant Physiol. **156:** 1808–1818.

Yamaguchi, M., Mitsuda, N., Ohtani, M., Ohme-Takagi, M., Kato, K., and Demura, T. (2011). VASCULAR-RELATED NAC-DOMAIN7 directly regulates the expression of a broad range of genes for xylem vessel formation. Plant J. **66:** 579–590.

Zuk, D., and Jacobson, A. (1998). A single amino acid substitution in yeast eIF-5A results in mRNA stabilization. EMBO J. **17:** 2914–2925.

Zuo, J., Niu, Q.W., and Chua, N.H. (2000). Technical advance: An estrogen receptor-based transactivator XVE mediates highly inducible gene expression in transgenic plants. Plant J. **24:** 265–273.